Journal of Power Sources 191 (2009) 384–389

Contents lists available at ScienceDirect

Journal of Power Sources

journal homepage: www.elsevier.com/locate/jpowsour

Long-term ageing and materials degradation of hybrid mica compressive seals for solid oxide fuel cells

Yeong-Shyung Chou*, J.W. Stevenson

K2-44, Energy Materials, Energy and Environment Directory, Pacific Northwest National Laboratory, P.O. Box 999, Richland, WA 99352, United States

ARTICLE INFO

Article history:
Received 13 January 2009
Received in revised form 16 February 2009
Accepted 17 February 2009
Available online 4 March 2009

Keywords:
Ageing
Thermal cycling
Leak rate
Mica seal
Phlogopite
SOFC

ABSTRACT

Hybrid phlogopite mica seals with silver interlayers were evaluated in long-term isothermal ageing tests in a dual environment consisting of dilute hydrogen versus air at 800 °C. High-temperature leak tests with helium showed very stable leakage of 0.01–0.02 sccm cm^{-1} for 28,366 h under a low applied compressive stress of 82 kPa (12 psi). Post-mortem SEM and EDS analyses of the mica showed minimum degradation in terms of changes in microstructure and chemical composition, although there appeared to be some Ag migration and segregation at interstices between mica flakes. Fluorine was also found to be released from mica. Overall, the low, constant leakage through the hybrid mica/Ag seals clearly demonstrated a very promising candidate for SOFC sealing.

1. Introduction

It is well recognized that sealing of planar solid oxide fuel cell (SOFC) stacks is one of the most challenging tasks for advancing SOFC technologies. The sealants have to survive numerous (up to thousands) of thermal cycles in the harsh SOFC environment and elevated temperatures. Hermeticity or allowable low leak rates are the first criterion for seal development. The sealant also have to demonstrate long-term (e.g., 40,000 h) stability in various aspects such as thermal, mechanical, electrical, chemical, and interfacial reaction. To date, there are three different approaches to SOFC seal development: rigid glass and/or glass–ceramic seals [1–4], compressive seals [5–7], and metallic active brazes [8]. Each approach has its own advantages as well as disadvantages as discussed in the review article by Fergus [9]. Among these approaches, compressive seals possess a very unique advantage in that no close match of the coefficient of thermal expansion (CTE) between adjacent SOFC components is required. Unlike other sealants, mica paper is composed of small, discrete mica flakes, ideally oriented with their cleavage planes parallel to each other. Since these mica flakes are not bonded to adjacent SOFC components such as interconnect plates or cell frame plates, no residual stresses would be expected to build up during thermal cycling.

The compressive mica seals have been studied extensively by the current authors in various aspects. In earlier studies, we identified the major leak paths of conventional compressive mica seals to be at the interfaces between the mating materials and the mica sheet, rather than through the mica seal itself [5,6]. Based on the findings, the "hybrid" mica seal was developed by adding two extra interlayers at these interfaces. The hybrid design resulted in reduction of high-temperature leak rates by 2–3 orders of magnitude as compared to the conventional mica seal [5,6]. The leakage could further be reduced when the interstices, i.e., voids, between mica flakes were filled with sealing glass [7]. However, the identification of a non-reacting glass with the required viscosity to fill the voids presented a challenge. Phlogopite micas were found to have reasonable thermal stability in air or a moist reducing environment [10]. Moreover, the hybrid phlogopite mica seal demonstrated excellent thermal cycle stability in open circuit tests over 1026 thermal cycles from ~100 to 800 °C in a moist reducing environment. The hybrid mica seal also showed good stability in combined ageing and thermal cycling in dual environments. In an earlier paper, we found constant leakage of ~0.02 sccm cm^{-1} (standard cubic centimeter per minute per centimeter of seal length) over a combined ageing of 4000 h and 119 thermal cycling for hybrid mica with silver as interlayers [11]. The effect of mica thickness was also reported; the leakage usually increased with increasing mica thickness [12]. More recent work on mica seals was focused on modeling of the effect of loading, slit geometry, and pressure difference [13], though the deformation and potential creep of mica which will change the slit geometry was not addressed. Attempts to modify the seal

* Corresponding author. Tel.: +1 509 375 2527; fax: +1 509 375 2186.
E-mail address: yeong-shyung.chou@pnl.gov (Y.-S. Chou).

0378-7753/$ – see front matter © 2009 Elsevier B.V. All rights reserved.
doi:10.1016/j.jpowsour.2009.02.052

microstructure were made by using fine alumina powders with Al particles [14], and fumed silica infiltrated ceramic fiber paper [15]. However, both approaches require higher compressive stresses to obtain leak rates comparable to hybrid mica seals. The use of metals such as Ag as a compressive seal was also investigated [16], but the issues of insulation, volatility, and cost need to be addressed. In this paper we will report recent results of very long-term isothermal aging studies of hybrid mica seals in the dual environment. High-temperature leak rates will be reported and material degradation will be characterized and discussed.

2. Experimental

2.1. Raw materials and hybrid mica seal preparation

The mica used in this study was a commercially available phlogopite mica paper with a thickness of about 100–200 μm (ultra high-temperature mica, McMaster-Carr, GA). Phlogopite mica ($KMg_3(AlSi_3O_{10})(F,OH)_2$) was selected due to its higher CTE ($\sim 11 \times 10^{-6}/^{\circ}C$) and thermal stability compared to muscovite mica ($KAl_2(AlSi_3O_{10})(F,OH)_2$, CTE $\sim 7 \times 10^{-6}/^{\circ}C$) [7,12]. The mica paper was composed of large, overlapping discrete mica flakes (hundreds to a thousand microns in size) with ~5 wt% of organic binder. For hybrid mica assembly, the phlogopite mica paper was cut into a 50 mm × 50 mm square ring with a central square hole of ~38 mm × 38 mm and sandwiched between two silver foils (25 μm thick and 99.95% pure, Alfa Aesar, MA) of similar size and shape. The width of the seal section was 5–6 mm. The hybrid mica assembly was then pressed between an Inconel600 square frame fixture (50 mm × 50 mm) and a flat substrate of as-received stainless steel (SS430), as shown in Fig. 1.

2.2. Isothermal ageing, leak test, and characterization

The long-term isothermal ageing of the hybrid mica seal was conducted at 800 °C with a constant applied compressive stress of 82 kPa (12 psi). The constant loading was applied by using dead weights from room temperature. The assembled hybrid micas were first slowly heated to ~500–600 °C for 2 h to burn off the organic binders, followed by heating to 850 °C for 1–2 h for silver interlayers to comply with the surface roughness, and then cooled to 800 °C for isothermal ageing. The hybrid micas were then exposed to a flowing reducing gas inside the Inconel600 test fixture and the outside and perimeter sections were exposed to ambient air (Fig. 1). Dilute hydrogen (~2.64% H_2/Ar + ~3% H_2O) was used as the fuel for the dual environment test. During isothermal ageing at 800 °C, the high-temperature leak rate was measured by switch from dilute hydrogen gas to ultra-high purity helium. The leak rate was determined by monitoring the pressure drop of a connected reservoir of known volume with time. The details of the leak rate calculation and experimental set up are given in Refs. [5,6]. In the current test, the pressure gradient (across the hybrid mica seal) for leak tests was 1.37 kPa (0.2 psi). After the test, the mica samples were detached from the Inconel600 test fixture and characterized with optical microscopy (OM) and scanning electron microscopy (SEM, JOEL SEM model 5900LV) with energy dispersive spectrometry (EDS) for elemental analysis. A cross-section of the sample was also cut, mounted, and polished to evaluate the materials loss of the silver interlayers.

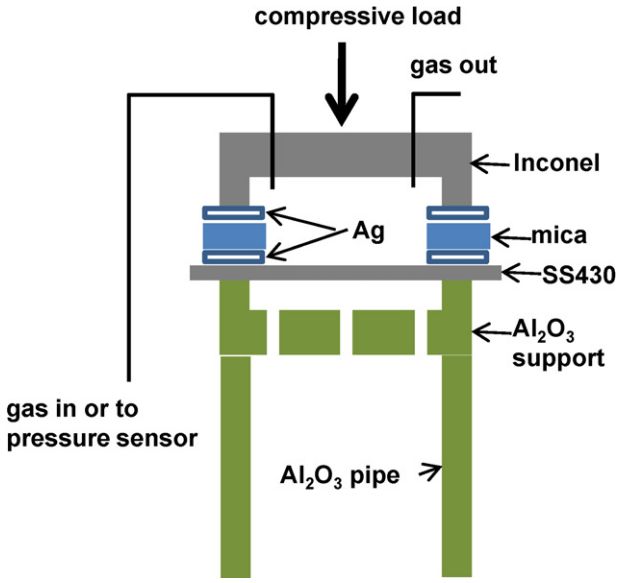

Fig. 1. Schematic of isothermal ageing and leak test set up where the hybrid mica with Ag interlayers was pressed between an Inconel600 (50 mm × 50 mm) block and a SS430 (1 mm thick) metal sheet at 82 kPa (12 psi). During ageing dilute hydrogen was flowing the upper chamber and He was used for leakage test.

3. Results and discussion

3.1. Leak rate during long-term isothermal ageing in dual environment

The 800 °C leak rates of the hybrid phlogopite mica seal with Ag interlayers are shown in Fig. 2. The leak rates were normalized with respect to the outer seal length (20 cm) of the square test fixture as standard cubic centimeters per minute per leak length, i.e., sccm/cm. Dilute hydrogen (~2.64% H_2/bal. Ar) containing a small amount of water (~3%) was used to provide a reducing atmosphere environment. The equilibrium PO_2 of this gas at 800 °C was calculated to be $\sim 5.8 \times 10^{-19}$ atm, which is in the typical PO_2 range for SOFC fuel environments at 800 °C ($\sim 10^{-21}$ to 10^{-16} atm). It was evident that the leak rates remained fairly constant between 0.01 and 0.02 sccm cm^{-1} during the first 3000 h of isothermal ageing. The leak rates slightly decreased to ~0.01 sccm cm^{-1} after ageing for about 8000 h. The measured leak rates were consistent with hybrid phlogopite micas using glass interlayers [11], and silver interlayers for the combined ageing and thermal cycling tests [12]. The reason for the slight improvement in leak rate is not clear. Given the fact that phlogopite mica is a layered aluminosilicate, the combination of high temperature and compressive stress may enhance or induce some creep behavior that could narrow the voids between discrete mica flakes, which were identified as the primary

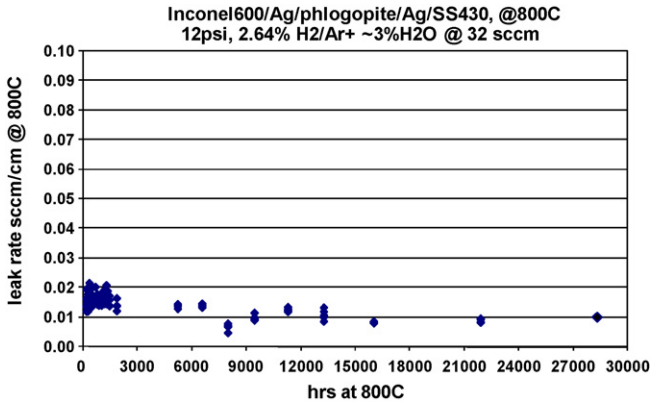

Fig. 2. Normalized leak rate of hybrid mica seal with Ag interlayers during long-term isothermal ageing at 800 °C in dual environment under 82 kPa (12 psi) compressive loading.

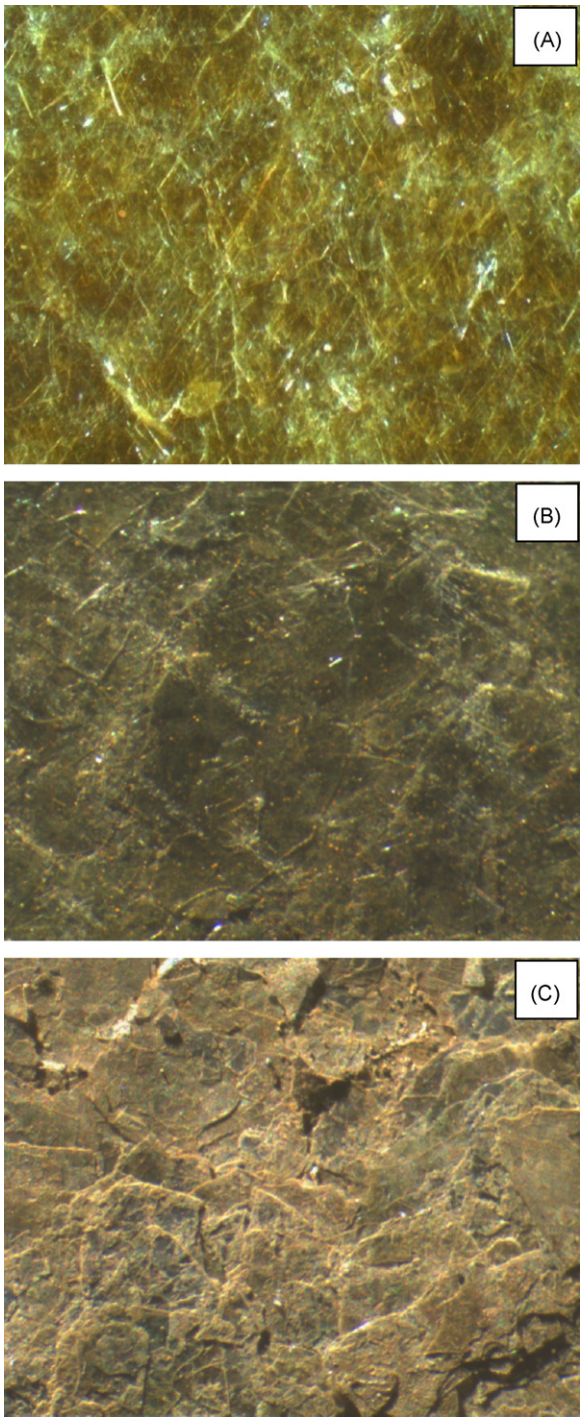

Fig. 3. Fracture surface morphology of hybrid mica after isothermal ageing test in a dual environment: (A) 0, (B) 1000, and (C) 28,366 h at 800 °C. Note that all fracture surfaces showed the typical flat cleavage planes of mica under optical microscopy, though there were some color differences.

leak paths if the interfaces were sealed with compliant Ag foil or glass [5].

3.2. Fracture surface and microstructure analysis

After completion of the long-term ageing test, the sample could be easily detached from the test fixtures, with fracture occurring along or near the silver/mica interface on the Inconel600 fixture side. Fig. 3 shows the fracture surfaces of the hybrid mica seal before (Fig. 3A) and after the long-term ageing test (Fig. 3C). A sample from a different test using the same materials that was terminated after a shorter ageing time (1000 h) is also shown for comparison (Fig. 3B). It is noted that the phlogopite mica turned into a golden color after the binder burn-off process in air, with shiny reflective fracture surfaces, indicating atomically smooth cleavage planes. After isothermal ageing for 1000 h in reducing environment, the golden color was no longer present; instead, the mica was gray-green or colorless. The surface still showed reflective cleavage planes (Fig. 3B). After 28,366 h of ageing, the mica appeared to be slightly brown in color and showed much less reflection on the fracture surface, though the presence of individual mica flakes was still discernable on the surface (Fig. 3C). The fracture surface features and coloring were consistent with a previous study of the same hybrid design with Ag interlayers which went through a combined ageing and thermal cycling test with an accumulation of 4000 h of isothermal ageing and 119 thermal cycles at 800 °C [12]. SEM analysis (Fig. 4A) showed the smooth cleavage planes of mica flakes overlapping with each other before the test. The 28,366 h aged sample showed a much rougher surface with many particles, though the mica flake morphology was still present (Fig. 4B). Under higher magnification, these particles were whitish in color, and EDS analysis confirmed they were Ag particles, likely formed by diffusion of Ag into voids between mica flakes from the interfaces, as shown in the cross-section view in Fig. 5.

It was mentioned above that, during post-test dis-assembly, fracture occurred along the silver/mica interface at the Inconel600 side rather than the interface at the SS430 side. This was expected due to the larger CTE mismatch between the hybrid mica and Inconel600 (CTE = 16–17 $\times$ 10^{-6}/°C) as compared to the bottom substrate (CTE = 12.5 $\times$ 10^{-6}/°C for SS430). The thin (25 μm) silver layer appeared strongly bonded to the Inconel600 fixture as well as to the SS430 substrates (1 mm thick), and would not change the CTE of the contact materials (Inconel600 and SS430) substantially. The thermal stability of phlogopite mica was further demonstrated by elemental analysis with EDS as shown in Fig. 6A–C for the mica before and after the long-term ageing test on the fracture surface and cross-section, respectively. It was evident that the major peaks (elements) remained the same in terms of relative intensities. For each sample, two areas were selected for elemental analysis and the results are listed in Table 1. It appears that the oxygen concentration was lower after the ageing test, although the EDS analysis was not very sensitive to oxygen detection. The presence of a small amount of Ag due to a diffusion/migration process was not surprising since the melting point of Ag is only 960 °C. Diffusion of Ag could potentially cause a problem if the Ag particles became connected to form a continuous electrical conduction path, which could lead to shorting through the seal. Careful evaluation of the fracture surfaces (Figs. 3C, 4C and 5) indicated that no continuous network of Ag particles formed. This issue can also be mitigated for actual planar SOFC stacks if the sealing areas on the metallic interconnects are covered with an insulating layer, e.g., Al_2O_3 [17].

3.3. Degradation of mica

It is important to know whether the sealing materials are durable enough to last for 40,000 h or more, which is the target life time for typical stationary SOFC applications. The fracture surface analysis described above indicated minimum physical degradations of the phlogopite mica during the isothermal aging. On the other hand, previous work has indicated degradation of phlogopite mica due to repeated frictional wear during thermal cycling. This was also observed in earlier studies of muscovite mica, in which, after 21 thermal cycles, the fracture surface showed many fragmented particles [10]. Addressing another aspect of physical degradation, our earlier study using thermogravimetric analysis showed the volatility (weight loss, likely due to the formation of

Table 1
Chemical compositions of hybrid mica before and after isothermal ageing (note for each sample two different areas were analyzed, and for aged sample both fracture surface and cross-section were analyzed).

Element at%	Area #1 Before	Area #2 Before	Area #1 Surface	Area #2 Surface	Area #1 Cross-section	Area #2 Cross-section
OK	51	52	43	42	43	42
FK	3.6	2.4	0.0	0.0	0.0	0.0
CrK	0.0	0.0	0.0	0.3	0.0	0.0
NaK	0.0	0.0	0.0	0.0	1.3	0.0
MgK	14	14	16	17	15	17
AlK	5.9	6.6	8.4	8.1	8.9	7.6
SiK	19	18	22	22	23	23
TiK	0.2	0.0	0.5	0.4	0.0	0.3
KK	5.2	5.5	6.0	5.6	5.1	7.6
FeK	1.4	1.7	3.0	3.1	1.8	1.7
AgL	0.0	0.0	1.3	1.5	2.0	0.6

gaseous $Si(OH)_4$) of phlogopite mica in humid (~30 vol.% H_2O) and reducing (~2.7% H_2/Ar) environments remained fairly constant at $\sim 1.6 \times 10^{-4}$ mg cm^{-2}-h @800 °C. The estimated total material loss for a 40,000 h operation was only ~0.5 wt%, which was deemed insignificant [11].

Fluorine was not detected by EDS after the ageing test in either the fracture surface or the cross-section. A few percent of fluorine was detected in the mica after heat-treatment at 800 °C for a few hours to burn off the organic binders (Table 1). Fluorine has long been recognized as a minor but significant constituent of hydrous minerals, such as mica and amphiboles [18]. Fluoride and hydroxyl ions have the same charge and are similar in size, so fluoride can exchange with hydroxyl in the mica's structure [19]. There are several species present in mica which can volatilize when mica is heated to high temperatures. Matson et al. [20] found the major volatile species for phlogopite mica heated in vacuum to 1300 °C was H_2O, which evolved in the temperature range of 1000–1150 °C. Our earlier TGA study showed a slightly lower initiation temperature for chemical water release: ~960 °C. Fluorine release trailed the high-temperature water release by ~50 °C and extended to above 1200 °C in some cases; the volatilization products consisted of both F and HF. Chlorine as Cl or HCl was typically released simultaneously with water [20]. After the long-term dual environment ageing in the present study, no fluorine was detected. The thermal stability and the mechanism of fluorine release from the mica's aluminosilicate layer structure in the reducing environment are not clear. However, F release has a potential impact to SOFC components if the fluorine comes off as HF in the fuel side where hydrogen is available. HF can be corrosive to the mica itself, which is a silicate mineral with a crystal structure consisting of combinations of an $(Si_2O_5)_n$ layer of SiO_4 tetrahedra joined at corners with an $AlO(OH)_2$ layer of alumina octahedra. It can also potentially react with the major components of silicate-based sealing glasses by the following reactions:

$$F_2(g) + H_2(g) \rightarrow 2HF(g) \quad (1)$$

$$SiO_2(s) + 4HF(g) \rightarrow SiF_4(g) + 2H_2O(g) \quad (2)$$

$$SrSiO_3(s) + 4HF(g) \rightarrow SrO(s) + SiF_4(g) + 2H_2O(g) \quad (3)$$

Simple thermodynamic calculations of Gibbs free energy versus temperature for these reactions were conducted and the results were plotted in Fig. 7 (the calculation used a commercial software of HSC Chemistry 5.11, Outokumpu, Finland). It is evident that the formation of HF by Eq (1) is very favorable, with a large negative free energy of −275 to −280 kJ mole^{-1} HF and very little temperature dependence for this spontaneous reaction (neglecting reaction kinetics). The reaction to form gaseous SiF_4 from mica (though the mica is not purely SiO_2 but a network of joined SiO_2 and $AlO(OH)_2$, the calculation serves as an estimation) appears to be less favorable with a very small negative free energy of ~4 kJ mole^{-1} at 800 °C. The free energy of this reaction is very dependent on temperature, as shown in Fig. 7. At temperatures above ~830 °C, the reaction would be thermodynamically unfavorable. As for reaction with the major crystalline phase of an alkaline-earth silicate sealing glass (e.g., $SrSiO_3$ in Sr–Ca–Y–B–Si glass [21]), the calculation showed a large positive free energy suggesting the attacking of HF on crystallized sealing glass would be unlikely. These alkaline earth silicate sealing glasses may still contain some residual glass even after long-term crystallization as a minor phase or along the grain boundaries [22]; however, degradation due to interaction with HF would likely be minimal due to the decreasing volume of these phases over ageing time. Another potential cause of degradation could be interaction between HF and ferritic stainless steel based interconnects. Most candidate steels for SOFC interconnect applications are chromia-formers, i.e., they form a protective chromia surface scale at elevated temperatures. Thermodynamic analysis indicated that, for an SOFC fuel gas containing, for example, 10 ppm HF, potential solid reaction products between HF and chromia, such as CrF_2, CrF_3, and CrF_4, are not thermodynamically favored to form, while formation of gaseous species containing Cr and F would be negligible (activities less than 10^{-21} atm). It should also be noted that ferritic stainless steel-based interconnects are sometimes provided with a protective alumina coating in the sealing area. For this case, thermodynamic calculations for reaction of HF and alumina to form AlF_3 indicated a large positive Gibbs free energy (~160 kJ mole^{-1} AlF_3), suggesting that no severe corrosion by HF would occur at aluminized surfaces. In recent "single cell stack" tests using hybrid Ag/mica seals together with a high-temperature alkaline-earth silicate sealing glass, no discernable degradation was observed on the cell's electrochemical performance when tested at 800 °C at 0.7 V for ~1500–2300 h. This may suggest any fluorine volatilized from mica as HF and/or reacted with glass to form SiF_4 in the reducing fuel environment was flushed out through the gas streams without having any adverse effects on cell performance. Detailed micro-analysis with transmission electron microscopy is underway to identify possible foreign species deposition at the active sites along the electrode/electrolyte triple phase boundaries.

3.4. Volatilization of silver interlayers

One other issue regarding the long-term durability of hybrid mica/Ag seals is the volatility of silver interlayers. Silver was chosen as the interlayer material because it is ductile, nonreactive to SOFC components, non-oxidizing, easy to process, and relatively inexpensive. However, silver does have a relatively low melting point of ~960 °C, considering the elevated operation temperatures for SOFCs. The material loss of pure silver in air and in reducing environments due to volatilization was studied by Meulenberg et al. [16]. They found that the vaporization rate was much greater in air than in the reducing environments; this was attributed to the volatilization of silver oxide and/or decomposition of the silver oxide. The

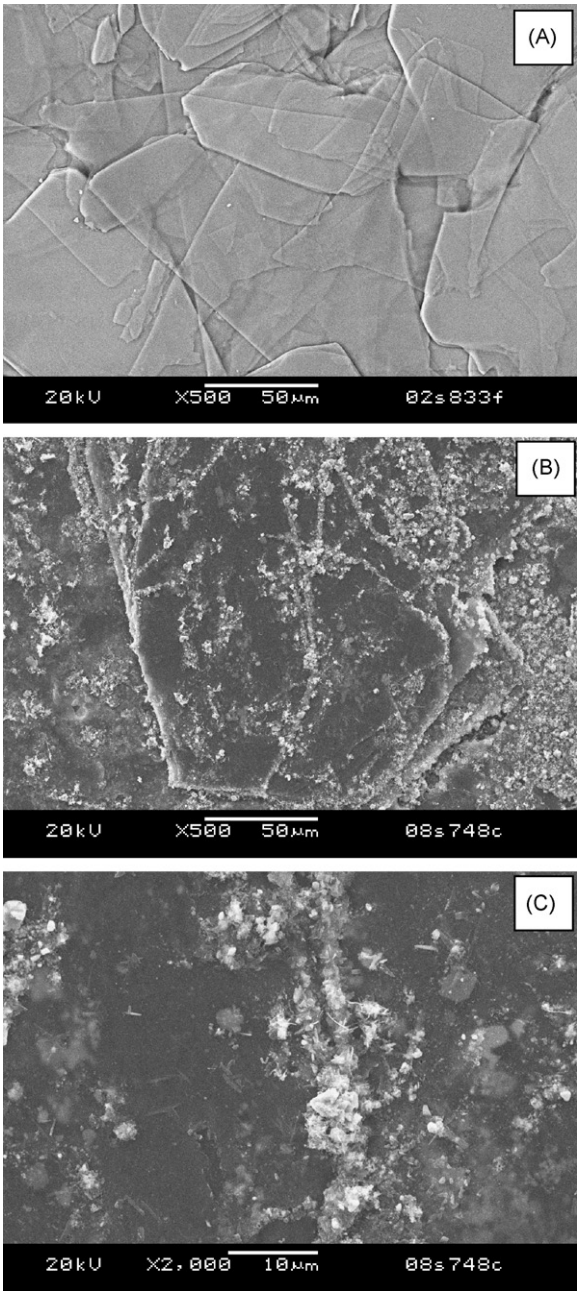

Fig. 4. Fracture surface morphology of hybrid mica after isothermal ageing test in a dual environment: (A) 0, (B) 28,366 h, and (C) a high magnification of (B). Note the fracture surface of aged sample showed discrete small white particles distributed along edges.

vaporization rate of pure silver (99.99% purity) in air was found to be 1.29×10^{-6} g cm^{-2}-h (790 °C) and the rate was 0.161×10^{-6} g cm^{-2}-h (800 °C) in 4% H_2/3% H_2O/bal Ar [16]. Using these data and simple flat plate geometry of Ag interlayers (pressed between mica paper and metal plates) with only exposed edges for vaporization, the estimated weight loss of silver interlayers from the air side was 0.98 and 0.12 wt% from the fuel side after 40,000 h at 800 °C [11]. From the cross-section of the pressed Ag/mica region (Fig. 8), it was evident the thickness of Ag (24–30 μm) was close to the initial nominal thickness (25 μm), consistent with our estimation of very small Ag loss over 40,000 h operation. It is also interesting to note that the Ag interlayers were very effective in blocking the diffusion of Cr and Fe from the metal parts in contact (Fig. 8), volatilization of the former is considered a major cause for degradation of cathode elec-

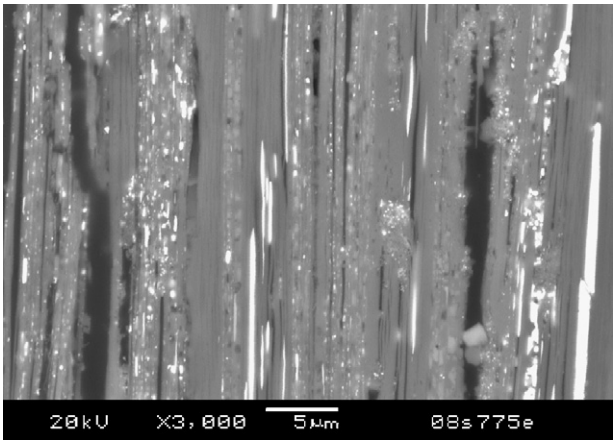

Fig. 5. Cross-section of hybrid mica seal after long-term ageing shows the penetration/migration of Ag (white phase) between mica flakes.

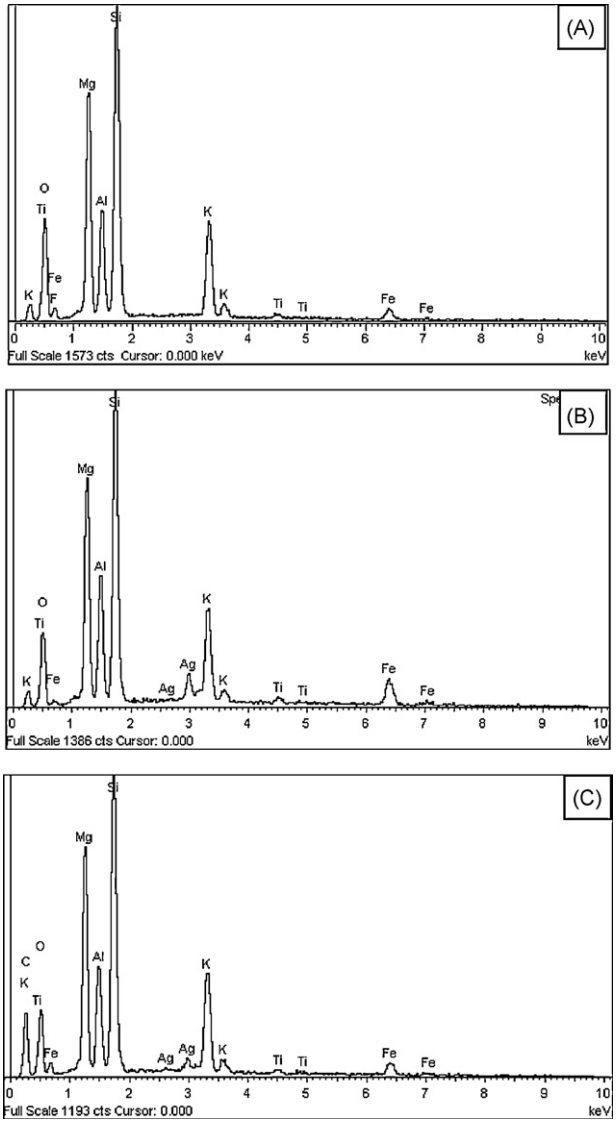

Fig. 6. Chemical analysis by EDS of the hybrid mica: (A) before isothermal aging from Ref. [11] and after 28,366 h from fracture surface (B), and from cross-section (C). The presence of Ag peak was due to atomic diffusion and migration at elevated temperatures. Overall the major peaks and relative intensities indicated minimum chemical composition changes after the long-term ageing test. The chemical compositions are listed in Table 1.

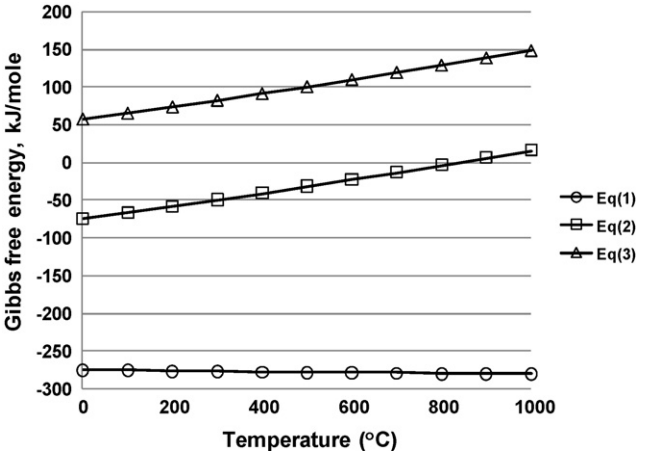

Fig. 7. Thermodynamic calculation of Gibbs free energy for reactions (1–3) versus temperature.

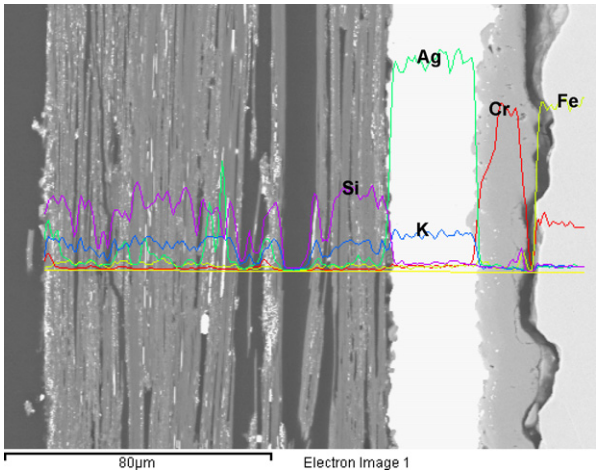

Fig. 8. Cross-section chemical analysis of hybrid mica with silver interlayer near the SS430 metal substrate. Note the penetration of Ag into the mica flakes and the effectiveness of Ag interlayer in blocking the diffusion of atoms from the substrate (Fe and Cr).

trochemical performance. The silver interlayer on the other hand was not effective in blocking oxygen diffusion, as the SS430 substrate eventually formed a thick Cr_2O_3 oxide layer, about 10–18 μm thick. Note that the observed crack along the Cr_2O_3 oxide layer and SS430 substrate was likely due to cutting and grinding processes during metallurgical sample preparation. Also note that there were several unexpected power failures during the long-term ageing test. The unexpected thermal cycles could cause the spallation of the Cr_2O_3 scale, leading to an increased leakage rate. The fairly constant leakage (Fig. 2) suggests that the thick Cr_2O_3 layer did not spall off the substrate. Overall, the simple material loss calculation, along with the observed Ag thickness and stable leak rates during long-term isothermal ageing clearly indicate the strong potential of hybrid Ag/mica seals for SOFC applications.

4. Conclusions

Hybrid phlogopite mica seals with silver interlayers were tested to evaluate their long-term thermal stability. Results of a 800 °C test over 28,366 h showed excellent thermal stability, with leak rates in the range of 0.01–0.02 sccm cm^{-1}, which is considered satisfactory for SOFC applications. Materials degradation of both mica and silver interlayers was characterized and discussed. It was found that the isothermal ageing caused no substantial physical degradation of mica. There was some penetration of silver into the mica paper; however, no continuous network of silver was formed to cause electrical shorting. EDS analysis confirmed the loss of fluorine from mica, thermodynamic calculations and experimental results suggested minimal effect on SOFC materials. Further characterization of silver interlayers also indicated that the loss of silver would be minimal for 40,000 h of operation. Overall, the hybrid phlogopite mica seal with silver interlayers proved to be a strong candidate for SOFC sealing applications.

Acknowledgements

The authors would like to thank S. Carlson for SEM sample preparation, and J. Coleman for SEM analysis. This paper was funded as part of the Solid-State Energy Conversion Alliance (SECA) Core Technology Program by the US Department of Energy's National Energy Technology Laboratory (NETL). Pacific Northwest National Laboratory is operated by Battelle Memorial Institute for the US Department of Energy under Contract no. DE-AC06-76RLO 1830.

References

[1] T. Yamamoto, H. Ito, M. Mori, N. Mori, T. Watanabe, Denki Kagaku 64 (6) (1996) 575–581.
[2] N. Lahl, D. Bahadur, K. Singh, L. Singheiser, K. Hilpert, J. Electrochem. Soc. 149 (5) (2002) A607–A614.
[3] K. Lye, M. Krumpelt, J. Meiser, I. Bloom, J. Mater. Res. 11 (6) (1996) 1489–1493.
[4] N. Lahl, K. Singh, L. Singheiser, K. Hilpert, J. Mater. Sci. 35 (2000) 3089–3096.
[5] Y.-S. Chou, J.W. Stevenson, L.A. Chick, J. Power Sources 112 (1) (2002) 130–136.
[6] Y.-S. Chou, J.W. Stevenson, L.A. Chick, J. Am. Ceram. Soc. 86 (6) (2003) 1003–1007.
[7] Y.-S. Chou, J.W. Stevenson, P. Singh, J. Power Sources 152 (2) (2005) 168–174.
[8] K.S. Weil, J.S. Hardy, J.Y. Kim, in: Joining of Advanced and Specialty Materials V, vol. 5, The American Society of Metals, 2002, pp. 47–55.
[9] J.W. Fergus, J. Power Sources 147 (2) (2004) 46–57.
[10] Y.-S. Chou, J.W. Stevenson, J. Power Sources 112 (2) (2002) 376–383.
[11] Y.-S. Chou, J.W. Stevenson, J. Hardy, P. Singh, J. Electrochem. Soc. 153 (2006) A1591–A1598.
[12] Y.-S. Chou, J.W. Stevenson, J. Power Sources 124 (2) (2002) 473–478.
[13] S. Sang, J. Pu, S. Jiang, L. Jian, J. Power Sources 182 (1) (2008) 141–144.
[14] S. Le, K. Sun, N. Zhang, Y. Shao, M. An, Q. Fu, X. Zhu, J. Power Sources 168 (2) (2007) 447–452.
[15] S. Sang, W. Li, J. Pu, L. Jian, J. Power Sources 177 (1) (2008) 77–82.
[16] W.A. Meulenberg, O. Teller, U. Flesch, H.P. Buchkremer, D. Stover, J. Mater. Sci. 36 (6) (2001) 3189–3195.
[17] Y.-S. Chou, J.W. Stevenson, P. Singh, J. Power Sources 185 (2) (2008) 1001–1008.
[18] J.L. Munoz, D.D. Ludington, Am. J. Sci. 274 (1974) 396–413.
[19] H.R. Westrich, Contrib. Miner. Petrol. 78 (1981) 318–323.
[20] D.W. Matson, D.W. Muenow, M.O. Garcia, Contrib. Mineral. Petrol. 93 (3) (1986) 399–408.
[21] Y.-S. Chou, J.W. Stevenson, P. Singh, J. Electrochem. Soc. 154 (7) (2007) B644–B651.
[22] K.D. Meinhardt, D.-S. Kim, Y.-S. Chou, K.S. Weil, J. Power Sources 182 (1) (2008) 188–196.